Original Paper *Forma*, **10**, 77–95, 1995

A Receptor Based Model for Pattern Formation in *Hydra*

J. A. SHERRATT[1,2], P. K. MAINI[2], W. JÄGER[3] and W. A. MÜLLER[4]

[1]*Nonlinear Systems Laboratory, Mathematics Institute, University of Warwick, Coventry CV4 7AL, U.K.*
[2]*Centre for Mathematical Biology, Mathematical Institute, 24-29 St. Giles', Oxford OX1 3LB, U.K.*
[3]*Institut für Angewandte Mathematik, INF 294, D-69120 Heidelberg, Germany*
[4]*Zoologisches Institut der Universität Heidelberg, INF 230, D-69120 Heidelberg, Germany*

(Received April 16, 1995; Accepted June 19, 1995)

Keywords: *Hydra*, Pattern Formation, Positional Value, Mathematical Models

Abstract. We propose a new theoretical model for pattern regulation in *Hydra*. Our model treats positional value and "head activation potential" as manifestations of the same cellular property, the amount of a regulatory biochemical bound to the cells *via* surface receptors. The model centres on the recently discovered interaction between the head- and foot-forming mechanisms, and we propose that both head and foot formation could be controlled by receptor-biochemical binding. Positional value is determined by the density of bound receptors, and polarity is established by a gradient in the number of receptors per cell. The local competition between cells for this biochemical regulator means that transplantation of tissue from a higher to a lower region of the body column causes an increase in the positional value of the transplanted tissue, at the expense of its new neighbours. We show that a local competition effect of this kind occurs if, in addition to the gradient in receptor density, there is also a gradient in the secretion rate of an enzyme that actively degrades the biochemical regulator. We show that with the combination of these two parallel gradients, the model is able to capture a wide range of results from cutting and grafting experiments. In particular, the model predicts that supernumerary heads induce the formation of supernumerary feet, whereas supernumerary feet do not induce new heads to form.

1. Introduction

The ability of the fresh-water polyp *Hydra* to regenerate lost body parts was recognised as early as the 18th Century (TREMBLEY, 1744). More recently, pattern formation in *Hydra* has been studied by many investigators (reviewed by BODE and BODE, 1984; MÜLLER, 1982, 1993). Normal development results in an animal with a head and foot at opposite ends of the body, interposed by a gastric region, budding zone and stalk (Fig. 1). However, simple cutting experiments demonstrate that all regions of the body are competent to form either a head or a foot, or any of the intermediate body parts. For example, after a transverse cut, the two resulting fragments form two intact animals, with

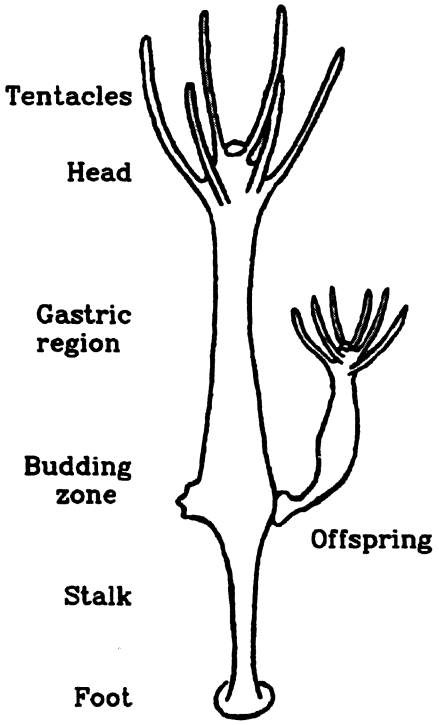

Fig. 1. A schematic illustration of *Hydra* anatomy. In cross-section, the body is tubular, with two concentric epithelial layers enclosing an interstitial space.

cells near the cut forming a head in one fragment and a foot in the other. Experiments of this kind strongly suggest that the cells respond to local positional cues that are dynamically regulated.

Further light is shed on this regulation by transplantation experiments, in which pieces of tissue are grafted from one animal to another (MACWILLIAMS, 1983a, b; MÜLLER, 1990). If the tissue is grafted to a position in the host that is nearer to the foot than its original location, a head tends to form; conversely, if the position in the host is nearer to the head than the original position, a foot tends to form. These results suggest that the origin of the positional cues is *local competition* for positional value (MÜLLER, 1990, 1994), with the ability to compete decreasing down the animal, from head to foot. Thus, when the grafted cells originate from nearer to the head end than the surrounding host cells, the grafted tissue is able to compete very successfully with the cells in its new surroundings. In comparison, in its original location, the tissue was less successful in this competition for positional value, since the cells to one side were better competitors. Therefore the grafted tissue will increase its positional value following transplantation. The reverse holds when the graft is from a region nearer to the foot. The same intuitive argument can account for the regenerative properties: the simple fact of being at the end of the animal means that cells are either the best or the worst competitors, and their positional value will then increase or decrease as a result. Throughout the paper we use the term "positional

value" rather than "positional information". In WOLPERT's (1969) original definitions, the latter term denotes a more labile property than the former; however, the schematic nature of our model makes it inappropriate to separate the two terms in the present context.

We propose a simple model for morphogenetic control in *Hydra*, based on this idea of local competition. Our model is based on the binding of a biochemical regulator to receptors on the surface of epithelial cells. Two theoretical models for pattern formation in *Hydra* have previously been proposed. WOLPERT *et al.* (1974) suggested a gradient model to account for head (but not foot) formation, in which a single diffusible chemical induces a head to form when its concentration falls below a critical, threshold value that decreases along the body column. This model builds on many previous qualitative discussions of the role of gradients in *Hydra* polarity and pattern formation (for example MORGAN, 1904; BURNETT, 1966), and although it is quite different from a formal point of view, the model we develop here can be thought of as further developing this gradient approach. A rather different type of model was proposed by H. Meinhardt and A. Gierer, based on local activation and long-range inhibition (GIERER and MEINHARDT, 1972; MEINHARDT and GIERER, 1974; GIERER, 1977; MACWILLIAMS, 1982; BERKING, 1984; MEINHARDT, 1993). Their model involves two or more diffusible morphogens, which regulate cellular differentiation; head-foot polarity is imposed by a gradient in the density of the sources of these morphogens. Each of the various body parts is assumed to be under the control of a separate activator-inhibitor system, coupled by the inhibitor production. The model we propose is quite different from the Gierer-Meinhardt model, and represents an alternative and rather simpler mechanism, whose predictions are also consistent with experimental observations.

The intense interest in *Hydra* development, both experimental and theoretical, is a function of its role as a paradigm for morphogenetic patterning. *Hydra* is one of the oldest and simplest organisms equipped with typically animal cells. Moreover, it exhibits a simple yet marked polarity in its body form. As such it reflects a pattern characteristic of many animal species. It is precisely this role of *Hydra* as a prototype for patterning that motivates the present study.

2. The Model

The basic idea behind our model is that the epithelial cells secrete a regulatory biochemical, which diffuses locally within the interstitial space and binds to receptors on the cell surface. We assume that there is a positive feedback loop between the density of bound receptors on the surface of a cell and the subsequent expression of new receptors on its surface. Such autocrine control of receptor expression is familiar from a number of other biological contexts (SKLAR *et al.*, 1984; NOJI *et al.*, 1991; MENDELSOHN *et al.*, 1991; ZIMMER and ZIMMER, 1992), and serves to amplify the local competition effects in our model. We also assume that the rate of biochemical secretion is uniform along most of the body column, but decreases in the foot; this decrease in secretion in the lower part of the body is motivated by specific experimental observations, as discussed below. We take positional value and "head activation potential" to be manifestations of the same cellular

property, namely the number of bound receptors on the cell surface. It is important to stress that our model does not depend on a juxtaposition of activation and inhibition; indeed there is no inhibitor in our model. This is not to say that an activator-inhibitor mechanism is not involved in *Hydra* morphogenesis. However, we consider the possibility of a local competition mechanism as the sole determinant of both head and foot formation.

We consider the possibility that local competition for positional value arises from a variation in receptor number and other parameters along the body column. It is important to stress that local competition could also arise in some other way, unconnected with chemical-receptor binding. Our model represents a detailed study of one possible mechanism for local competition. One simple measure of the variation in model parameters along the body column is the equilibrium values of biochemical concentration, and of free and bound receptors per cell, that would be implied by the binding kinetics in the absence of biochemical diffusion. These equilibrium levels are purely functions of the reaction kinetics governing cell-receptor production and binding.

In order to achieve the required local competition phenomenon, we suppose that the diffusionless equilibrium value of biochemical concentration increases along the body column, while the values of bound and free receptor numbers are roughly constant. Biochemical diffusion will tend to homogenise the varying diffusionless equilibrium concentration of chemical, and the effect of this will be to induce a decrease in bound receptor density down the body column. We show in the Appendix that a natural way in which such variations in the diffusionless equilibrium values can occur is for both the number of receptors per cell and the decay rate of free biochemical to decrease along the body column. This achieves precisely a local competition effect for the biochemical amongst cell surface receptors, due to local extracellular diffusion of the chemical. Biologically, a gradient in receptor density can easily be accounted for as a simple variation in cell phenotype. However, a gradient in biochemical decay rate requires more explanation, and we assume that the cells secrete an enzyme that degrades the biochemical, with the secretion rate decreasing along the body column. Although such an enzyme will diffuse along the body column, this is not crucial to the model mechanism. Rather, the role of the enzyme is to remove the biochemical regulator before it binds to the receptors on the cell surface. A variation in the rate of internalization, for example, would not be equivalent because it would affect biochemical and receptors in the same way.

These are the key ingredients of our model, which is illustrated schematically in Fig. 2. The mathematical formulation is discussed in the Appendix, and consists of conservation equations for extracellular biochemical, free receptors, bound receptors, and degradive enzyme. It is important to stress that the particular equations we choose are not of great significance. We use a mathematical representation simply as a tool to help clarify our ideas and explore their implications, and many other mathematical representations would work equally well. A number of previous authors have proposed receptor based models for the evolution of spatial pattern, in particular for the formation of cAMP patterns in *Dictyostelium* cells (MARTIEL and GOLDBETER, 1987; MONK and OTHMER, 1989; HÖFER *et al.*, 1994). The simplicity of our model compared to these detailed and rather specific

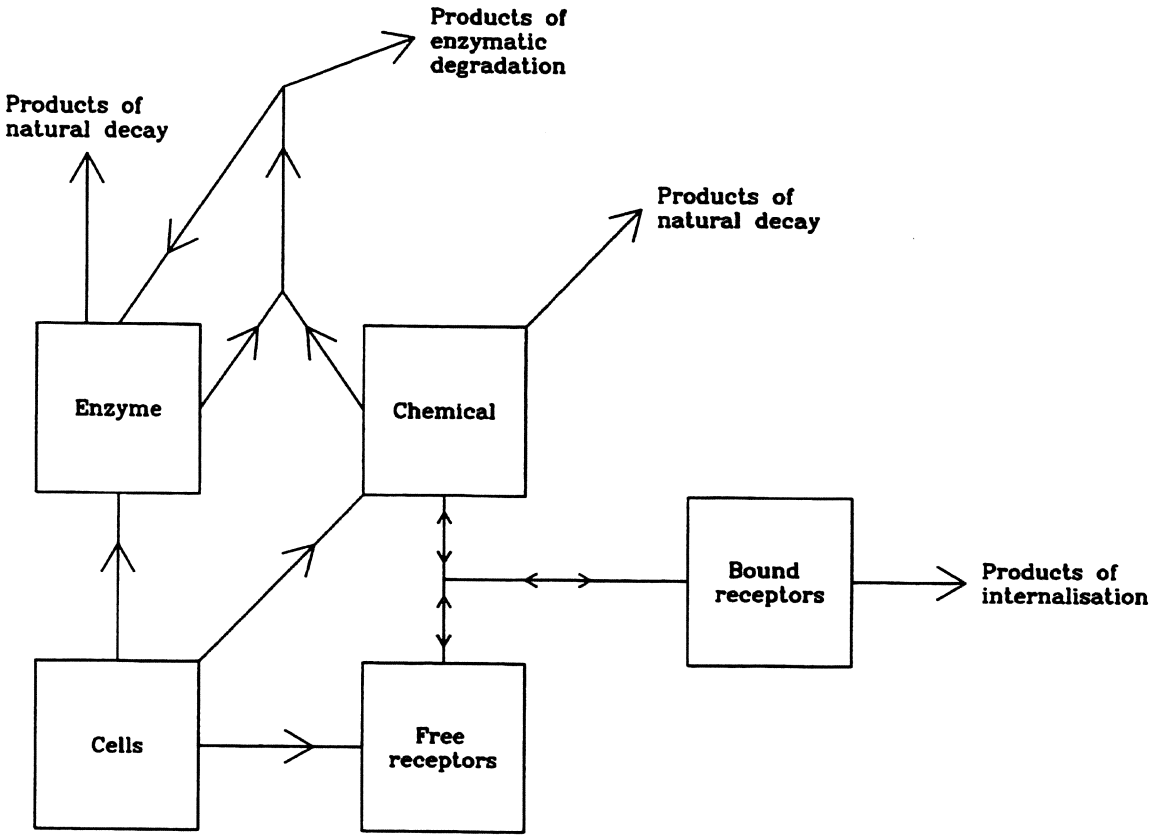

Fig. 2. A schematic illustration of our mathematical model, which is described in full in Appendix. In our model scheme, epithelial cells secrete a biochemical and an enzyme that degrades this biochemical, and also produce free receptors onto the cell surface, at a rate that increases with the proportion of receptors that are occupied. The free receptors reversibly bind extracellular biochemical, and the bound receptors are internalised within the cell, generating waste products. Both biochemical and enzyme undergo natural decay. In order to generate an appropriate local competition phenomenon, we assume that the rates at which the cells produce receptors and enzyme both decrease along the body column.

schemes is largely a reflection on the absence of detailed knowledge of the biochemical details of pattern control in *Hydra*.

The model solution corresponding to normal development in *Hydra* is illustrated in Fig. 3. We assume that a single positional value (namely the density of bound receptors) dictates the patterns underlying both head and foot formation. This is in keeping with recent experimental evidence for the interaction between the head- and foot-forming mechanisms (ANDO *et al.*, 1989; MÜLLER, 1989, 1990, 1994), and is a major conceptual difference between our model and that of Gierer-Meinhardt, in which a separate activator-inhibitor system regulates the formation of each body part. To be specific, we assume that in normal development the upper and lower quarters of the body column constitute the head and foot respectively; the model solution illustrated in Fig. 3 then enables us to read off the threshold values of bound receptor density for head and foot formation. We can

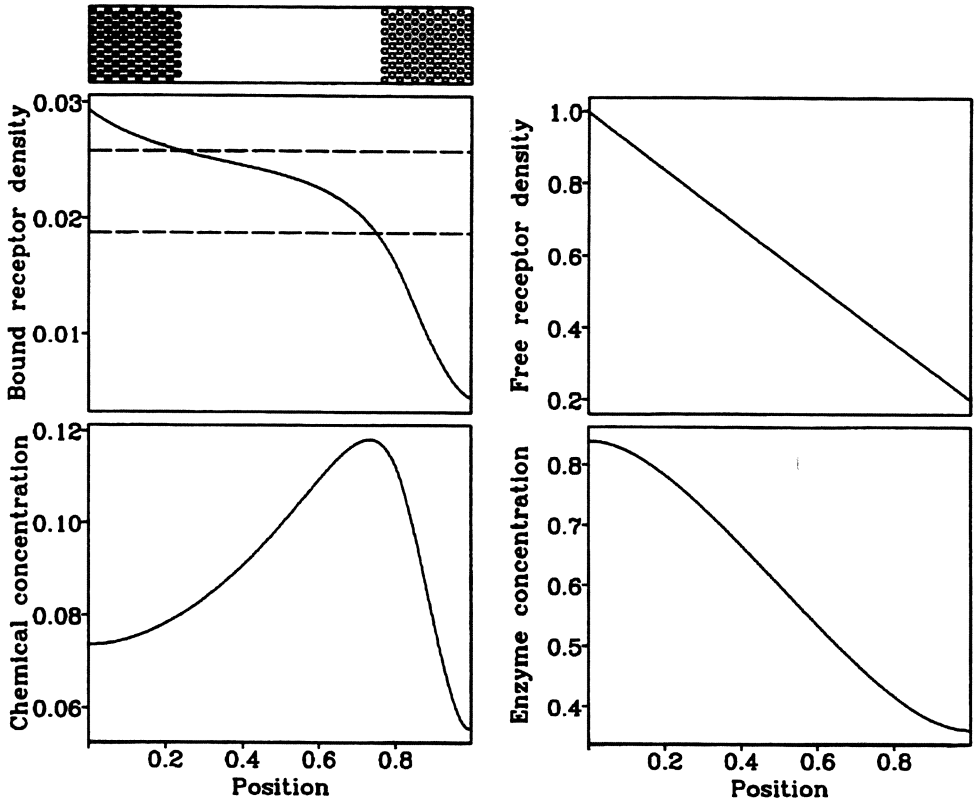

Fig. 3. The model solution corresponding to normal development. We denote schematically the head (●) and foot (○) regions. We also plot the solutions for chemical and enzyme concentrations, and free and bound receptor densities. It is the bound receptor density that determines positional value, and we use dashed lines to indicate our assumed threshold levels for head and foot formation. The mathematical formulation of the model, parameter values and method of numerical solution are all described in the Appendix.

then use these threshold values to make specific predictions concerning head and foot formation in the simulations of cutting and transplantation experiments discussed below. It is important to stress that the parameter values used in Fig. 3 and in all subsequent model simulations are estimated as far as possible from available data, as described in the Appendix. There is no fitting of parameters to match experimental results in any of our simulations.

3. Simulation of Cutting and Transplantation Experiments

We have solved the model equations to simulate the main cutting and grafting experimental phenomena associated with *Hydra*. The phenomena are listed below, together with experimental references and the number of the figure showing the corresponding model solution. In each case, the model solutions agree very well with the experimental observations.

1. The head and foot regenerate when they are cut off (TREMBLEY, 1744; WEBSTER

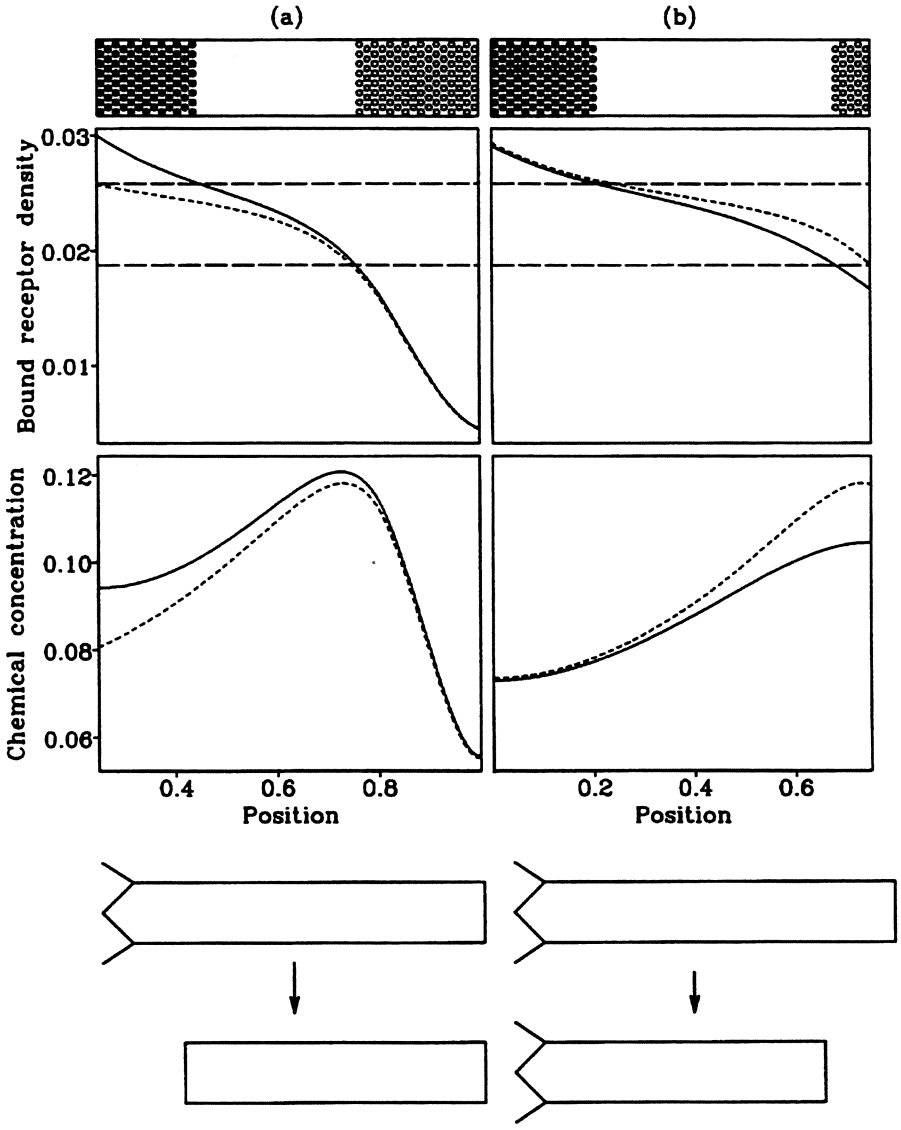

Fig. 4. The solutions of the model corresponding to surgical removal of (a) the head and (b) the foot. In both cases, the structures regenerate. Because part of the tissue has been removed, the position variable x ranges from 0.25 to 1 in (a), and 0 to 0.75 in (b), compared to 0 to 1 in normal development. (This is explained more fully in the Appendix.) In addition to our schematic illustration of the head (●) and foot (○) regions, we plot the variation in bound receptor density (which determines positional value) and biochemical concentration along the body column (—). We also plot the corresponding variations in the corresponding regions of a control animal, in which normal development has occurred (- - -), and we indicate our assumed threshold levels of bound receptor density for head and foot formation (– – –). The mathematical formation of the model, parameter values and method of numerical solution are all described in Appendix. Here and in other figures representing the model simulations of cutting and transplantation experiments, we include schematic representations of the experiment being simulated.

and WOLPERT, 1966; BODE and BODE, 1984). This is reflected in our model solutions (Fig. 4) because the positional value at the point just below the head in a normal animal is suppressed by the cells of the adjacent head, which are better competitors due to their higher receptor density. Decapitation removes this suppressive effect and the positional value of the cells at the new free end increases accordingly. The foot regenerates for corresponding reasons.

2. Transplantation of tissue from parts of the body column nearer to the head/foot induces head/foot formation (WEBSTER and WOLPERT, 1966; MACWILLIAMS, 1983a, b; MÜLLER, 1990). Within the context of the model, when a tissue is transplanted further up the body column than its original position (nearer the head) the transplanted cells are significantly worse competitors than those of the surrounding tissue in the new environment. Thus the positional value of the transplanted tissue decreases due to the transplantation, resulting in foot formation, while that of the surrounding tissue increases slightly (Fig. 5).

In experimental studies, one measures a *frequency* of head/foot formation. That is, the same transplantation experiment does not always give the same result, due to differences between individual animals. In contrast our model is purely deterministic, and the same "theoretical experiment" always gives the same result. This result corresponds to a prediction of the average result from actual experiments. A crucial feature of the average results of transplantation experiments is that the frequency of new head/foot formation increases with the distance between the original and new sites of the graft. The above explanation suggests that this observation should be reflected in the model solutions, and this is confirmed in Fig. 6.

3. Transplantation of additional heads periodically along the body column induces feet to form between the heads (MÜLLER, 1989, 1990). This is reflected in model solutions (Fig. 7a), since after the transplantation the tissue between the new heads is surrounded by much better competitors, and its positional value is greatly reduced as a result. However, experiments show that heads do not form between supernumerary feet (MÜLLER, 1989, 1990). The model reflects this phenomenon too (Fig. 7b), but this depends crucially on the reduced level of biochemical secretion in the lower part of the body column. If the secretion rate is taken to be uniform along the whole of the body column, including the foot, then the model predicts that transplantation of feet does induce head formation, in the same way as heads induce foot formation. However the combination of reduced biochemical secretion rate within the transplanted tissue and local biochemical diffusion counteracts the increase in positional value in regions adjacent to the transplanted feet, and prevents head formation.

Figure 7 illustrates the phenomenon of the long range suppression of competitive head formation by the existing host head: the peaks become higher as the distance from the host head increases, corresponding to a higher probability and speed of head formation. In all previous models, this suppression is achieved by the secretion of a long range inhibitor. Such an inhibitor may certainly exist, but an interesting and novel feature of our scheme is that the suppression phenomenon occurs even in its absence.

In Figs. 4, 5 and 7, there is a sharp division in positional value between the transplanted tissue and the surrounding host tissue, due to the sudden change in cellular

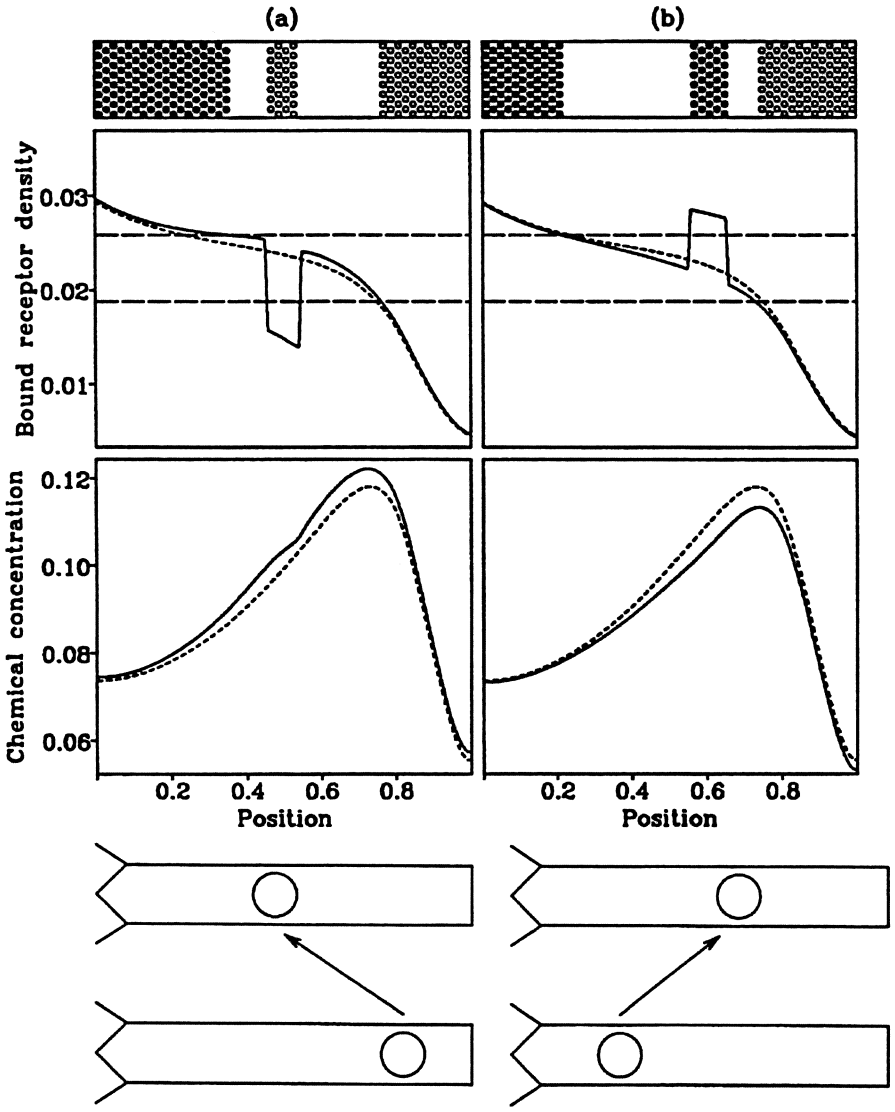

Fig. 5. Solutions of the model corresponding to transplantation experiments. (a) Transplantation of a 0.5 mm long region of tissue (10% of the body column length) from a position 80% along the body column (from head to foot) to a position 50% along a host animal, resulting in the formation of a new foot. (b) A reverse transplantation, from 40% along the body column to 60% along a host, resulting in a new head. In addition to our schematic illustration of the head (●) and foot (○) regions, we plot the variation in bound receptor density (which determines positional value) and biochemical concentration along the body column (—). We also plot the corresponding variations in a control animal (- - -), and we indicate our assumed threshold levels of bound receptor density for head and foot formation (– – –). The mathematical formulation of the model, parameter values and method of numerical solution are all described in the Appendix.

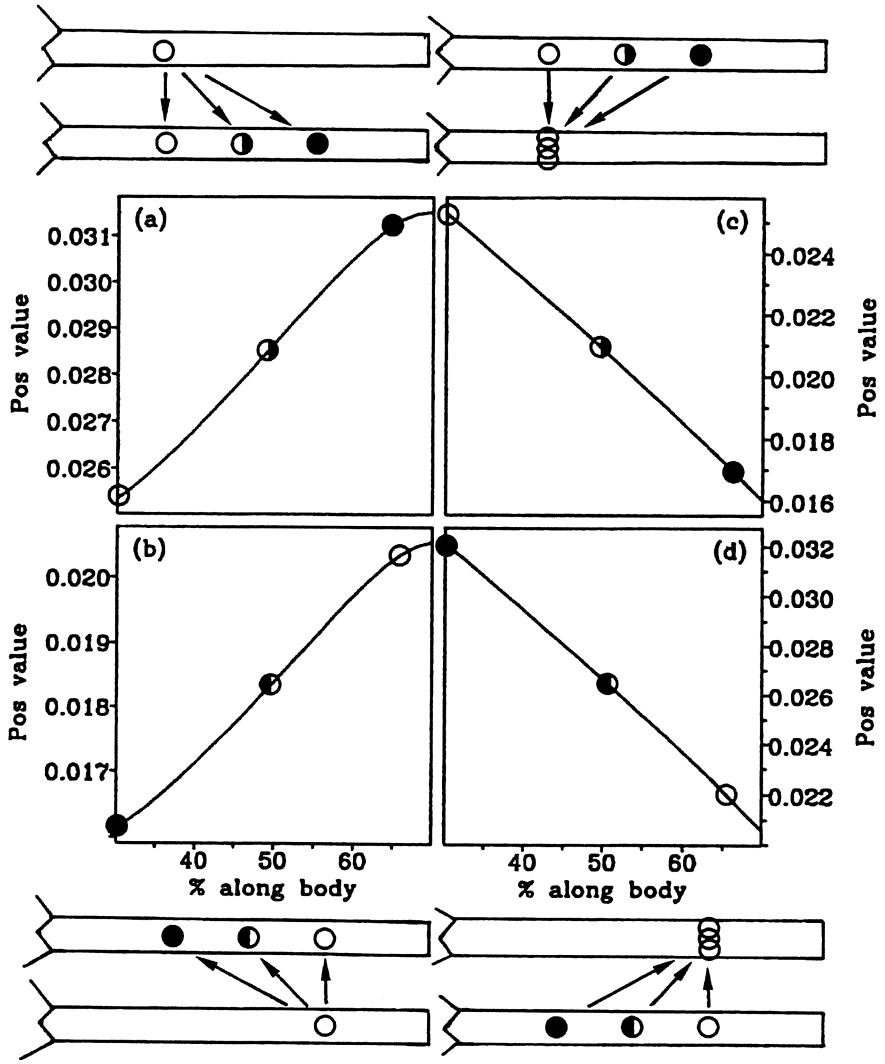

Fig. 6. The model prediction of the effects of tissue location within host and donor animals on the results of transplantation experiments. The figures show the predicted final positional value at the center of the transplanted tissue. (a) The position in the donor is 30% along the body column (from head to foot), and the position in the host is varied. (b) The position in the donor is 70% along the body column, and the position in the host is varied. (c) The position in the host is 30% along the body column, and the position in the donor is varied. (d) The position in the host is 70% along the body column, and the position in the donor is varied. Explanatory sketches are added beside each figure part for the purposes of clarity. In each case the region of tissue transplanted is 10% of the body column length. The model prediction of positional value at the center of the graft can be taken as a measure of the predicted frequency of head (high values) and foot (low values) formation in actual experiments, and thus the trends are exactly those found in experimental studies (MACWILLIAMS, 1983a, b; MÜLLER, 1990).

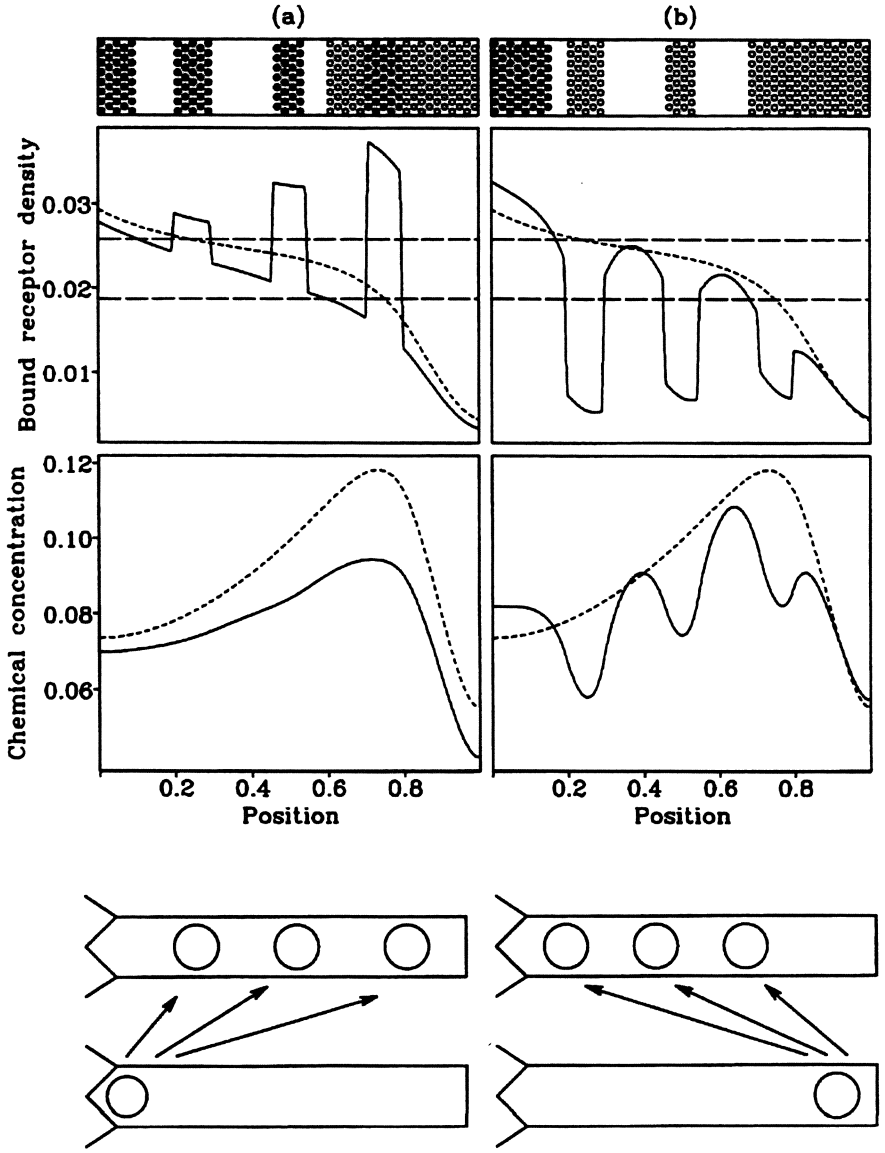

Fig. 7. Solutions of the model corresponding to the transplantation of (a) additional heads, and (b) additional feet, periodically along the body column. The new heads induce the formation of additional feet, but new feet do not induce additional heads to form. Note that in (b), the bound receptor density between the feet is no higher than in a control animal. In addition to our schematic illustration of the head (●) and foot (○) regions, we plot the variation in bound receptor density (which determines positional value) and biochemical concentration along the body column (—). We also plot the corresponding variations in a control animal (- - -), and we indicate our assumed threshold levels of bound receptor density for head and foot formation (– – –). The mathematical formation of the model, parameter values and method of numerical solution are all described in the Appendix.

properties. In reality, a sharp division forms initially, and gradually smooths out over days or weeks, due at least in part to the growth of the animal. However, we do not expect a schematic model such as ours to be able to capture this level of biological detail.

Finally we comment that our model does not address the possibility of bud formation. Simple observations show that the appropriate positional value for bud formation is that between the foot and gastric region in a normal animal. However buds form with very variable frequencies, and in addition to positional value, bud formation is also regulated by a number of factors not directly related to mechanisms of pattern generation such as body size, availability of resources and active tissue movement (CAMPBELL, 1967; BERKING, 1977; ANDO *et al.*, 1989; MEINHARDT, 1993; MÜLLER, 1995a, b).

4. Discussion

We have described a mechanism for pattern formation in *Hydra*, in which positional value is determined by the density of bound receptors for a single regulatory biochemical. Spatial structure arises because of local competition for this regulator. The very good agreement between the model predictions and the results of a number of key experiments suggests that a mechanism of this general type is a plausible candidate for pattern regulation in *Hydra*. It is important to stress that our model is not a mechanism for *de novo* pattern formation. Rather, we impose an initial gradient in receptor number, and suggest a mechanism by which this is transformed into the observed morphological pattern. Such hierachies of pattern were an integral part of TURING's (1952) original scheme for diffusion-driven pattern formation, and have recently been proposed as an important regulator of chondrogenesis in the vertebrate limb (MAINI *et al.*, 1992; BENSON *et al.*, 1993).

We have discussed in detail the model simulations of cutting and grafting experiments. However, there are several other key experimental results on *Hydra* morphogenesis of a rather different type, which we now discuss. About 20 years ago, GIERER *et al.* (1972) and NODA (1971) showed that normal *Hydra* can regenerate from random cellular reaggregates; this regeneration occurs without cell sorting with respect to the positional origin of the cells along the body axis (SATO *et al.*, 1992; TECHNAU and HOLSTEIN, 1992). More recently, ANDO *et al.* (1989) succeeded in grafting together ring-shaped pieces of tissue ("tandem grafts") excised from the same position on different animals. The resulting homogeneous tube formed a series of heads, buds and feet. It is clear that neither of these results would be predicted by the model we have discussed: in both cases the model predicts essentially no spatial structure. In particular, the model solutions do not have any tendency towards increased pattern complexity as the domain length increases; this is because in contrast to previous models we are not assuming a superposition of short and long range interactions.

Another important experimental result is the ability of protein kinase C activators such as diacylglycerol (DAG) to induce ectopic head formation without surgery (MÜLLER, 1989, 1990). Following repeated daily treatments with DAG, additional ectopic heads form along the body length. This occurs only after a week or more of daily treatments, but after a shorter time, there is a general increase in the positional value. This can be seen in

the fact that transplantation of a region of tissue from a DAG treated animal to the same position in an untreated animal generally results in head formation after just a few days of DAG treatment. Within the context of our model, it seems natural to suggest (MÜLLER, 1995a, b) that DAG treatment results in additional secretion of the biochemical regulator by the epithelial cells. As one would expect, this tends to increase the positional value at all points along the body column, which is broadly in keeping with the experimental results. However, the model is unable to account for the observed strain-specific locations of supernumerary head structures that result from DAG treatment.

Several modifications and extensions of our model enabling it to generate patterns *de novo* can be envisaged, and we anticipate that the shortcomings of our model would be resolved by an appropriate extension of this type. However, in the absence of detailed knowledge of the actual biochemical mechanisms, such extensions run a high risk of being unrealistic.

JAS was supported in part by a Junior Research Fellowship at Merton College, Oxford. PKM would like to thank the Robert F. Philip Endowment for support and the Department of Applied Mathematics, University of Washington, Seattle for its hospitality.

APPENDIX

In this appendix we outline the mathematical formulation of our model, which is illustrated schematically in Fig. 2. We denote the concentrations of biochemical and degradive enzyme by $a(x, t)$ and $e(x, t)$ respectively, where x and t are space and time coordinates, with x increasing from 0 to L along the body column. The bound and free receptor densities are denoted by $b(x, t)$ and $f(x, t)$ respectively. For simplicity, we assume that all binding processes are governed by the law of mass action, without any saturation effects. We must also specify the rate of production of new free receptors at the cell surface, and following SHERRATT *et al.* (1993), we suppose that the production rate is such that at equilibrium, the total number of receptors on the cell surface increases linearly with the number of bound receptors, with the form $b+f=\alpha+\beta b$. Here α and $\beta(<1)$ are positive parameters; α is the number of receptors on an unstimulated cell, while $\alpha/(1-\beta)$ is the saturating receptor density at very high biochemical concentrations. Our assumption that the availability of receptors decreases along the body column implies that α and possibly also β are functions of tissue location. To be specific, we take α to decrease linearly along the body column, while β is constant. However, very similar results are obtained if β also decreases.

Our model equations have the following form:

$$\frac{\partial a}{\partial t} = D_a \frac{\partial^2 a}{\partial x^2} + s_a(x) - \mu_a a - k_e ae - k_a af + k_d b, \tag{A1a}$$

$$\frac{\partial f}{\partial t} = k_d b - k_a af + k_i\left[\alpha(x) + \beta b - f\right], \tag{A1b}$$

$$\frac{\partial b}{\partial t} = k_a af - (k_d + k_i)b, \tag{A1c}$$

$$\frac{\partial e}{\partial t} = D_e \frac{\partial^2 e}{\partial x^2} + s_e(x) - \mu_e e \tag{A1d}$$

where $\alpha(x) = \alpha_1[1 - y(x)/L] + \alpha_2 y(x)/L$, $s_e(x) = s_1[1 - y(x)/L] + s_2 y(x)/L$. The interpretation of the various parameters is summarised in Table A1. The spatial variable x denotes position along the body column, with $x = 0$ and $x = L$ corresponding to the head and foot ends respectively. The function $y(x)$ the denotes position from which the tissue at location x originates. In normal development, $y(x) = x$; however, $y(x)$ differs from x in the various cutting and grafting experiments considered in the main body of the paper. Within the context of the model, it is the form of $y(x)$ that determines the experimental situation, and in Table A2, we list the expressions for $y(x)$ that were used in the numerical solutions illustrated in Figs. 3–5 and 7. The secretion rate $s_a(x)$ is constant on $0 < y(x) < 4L/5$, and for simplicity we assume that it decreases linearly to zero on $4L/5 < y(x) < L$. However, the form of this decrease is not at all crucial, and the model solutions have essentially the same qualitative form even if we take s_a to be identically zero on $4L/5 < y(x) < L$. We assume zero flux boundary conditions on the biochemical concentration a and the enzyme concentration e; no boundary conditions are required for b and f. Note that in the absence of diffusion, the equilibrium values implied by the above kinetics are: $e = s_e(x)/\mu_e$, $f = \alpha(x) - (1 - \beta)b$, $a = [s_a(x) - k_i b]/[\mu_a + k_e s_e(x)/\mu_e]$, where b is the unique solution of $(k_d + k_i)b/[k_a(s_a(x) - k_i b)] = [\alpha(x) - (1 - \beta)b]/[\mu_a + k_e s_e(x)/\mu_e]$. Since s_a is constant along most of the

Table A1. A summary of the interpretations of the dimensional model parameter values.

Parameter	Interpretation
D_a	Biochemical diffusion coefficient
s_a	Rate of biochemical secretion by cells
μ_a	Biochemical decay rate
k_e	Reaction rate of enzyme-catalysed biochemical degradation
k_a	Association rate of biochemical and free receptors
k_d	Dissociation rate of bound receptors
k_i	Internalisation rate of bound receptors (resulting in intercellular degradation)
α_1	Unstimulated receptor density at head end
α_2	Unstimulated receptor density at foot end
β	$1/(1 - \beta)$ is the factor by which the total receptor density increases in a maximally stimulated cell
D_e	Enzyme diffusion coefficient
s_1	Secretion rate of enzyme by cells at head end
s_2	Secretion rate of enzyme by cells at foot end
μ_e	Decay rate of enzyme

Table A2. The dimensional functional forms for $y(x)$ and the ranges of x that were used in the model solutions illustrated in Figs. 3–5 and 7. The function $y(x)$ reflects the position along the body column of the original location of the tissue at position x.

Figure	$y(x)$		Range of x
3	x		$0 \leq x \leq L$
4a	x		$L/4 \leq x \leq L$
4b	x		$0 \leq x \leq 3L/4$
5a	$x + 0.3L$	when $\lvert x/L - 0.5\rvert < 0.05$	$0 \leq x \leq L$
	x	otherwise	
5b	$x - 0.2L$	when $\lvert x/L - 0.6\rvert < 0.05$	$0 \leq x \leq L$
	x	otherwise	
7a	$x - 0.2L$	when $\lvert x/L - 0.25\rvert < 0.05$	$0 < x < L$
	$x - 0.45L$	when $\lvert x/L - 0.5\rvert < 0.05$	
	$x - 0.7L$	when $\lvert x/L - 0.75\rvert < 0.05$	
	x	otherwise	
7b	$x + 0.7L$	when $\lvert x/L - 0.25\rvert < 0.05$	$0 < x < L$
	$x + 0.45L$	when $\lvert x/L - 0.5\rvert < 0.05$	
	$x + 0.2L$	when $\lvert x/L - 0.75\rvert < 0.05$	
	x	otherwise	

body column, while s_e and α decrease significantly and in parallel, the diffusionless equilibrium value of b is fairly constant along the body column, while that of a increases significantly. It is these variations that enable our model to exhibit the appropriate type of local competition.

A.1. Parameter values

The body length of *Hydra*, L, is typically about 5 mm. However, there is no specific data to enable any of the other model parameters to be determined, since particular biochemicals which regulate pattern formation have not been identified. We now present some simple calculations which help to suggest the likely orders of magnitude of the model parameters.

1. The half lives for decay of extracellular biochemical and degrading enzyme are $\log 2/\mu_a$ and $\log 2/\mu_e$ respectively. We can reasonably expect both these half lives to be about an hour, giving $\mu_a \approx \mu_e \approx 2 \times 10^{-4}\ \mathrm{s}^{-1}$.

2. We assume that the half life of occupied receptors on the cell surface, with respect to both dissociation and internalization, is about one tenth that of extracellular biochemical, which gives $k_d \approx k_i \approx 2 \times 10^{-3}\ \mathrm{s}^{-1}$. These are about half the values of the corresponding rate constants for occupied receptors for N-formylated peptide chemoattractants on the surface of neutrophils (SKLAR *et al.*, 1984). If we take k_a to be also about half the value in the neutrophil-peptide system, we have $k_a \approx 10^4\ \mathrm{M}^{-1}\mathrm{s}^{-1}$.

3. We expect that when e has its maximum diffusionless equilibrium value of s_1/μ_e, the rate of enzymatic degradation is at least an order of magnitude greater than the rate of natural decay, and thus we take $k_e \approx 15\ \mu_a\mu_e/s_1$.

4. MACWILLIAMS (1983b) has suggested that a diffusible pattern regulator in *Hydra* will have a half life of about 2×10^{-6} cm^{2}s^{-1}. This is a reasonable value for the diffusion coefficient of a fairly small biochemical *in vivo* (SHERRATT and MURRAY, 1990; SHERRATT, 1994), and we take it to be the value of D_a. We assume that the enzyme diffuses at about the same rate.

5. In the well studied neutrophil-peptide system, it is known that an unstimulated cell has about 3000 receptors on its surface, and that binding of ligand to these receptors can increase this number by as much as 10 fold. We assume that the receptor density on the epithelial cells in *Hydra* will be about the same, with the unstimulated level varying by a factor of 5 along the body column. Therefore we take $\alpha_2 = 800$/cell, $\alpha_1 = 4000$/cell and $\beta = 0.9$. We also assume that s_e decreases by the same factor of 5 along the body column, so that $s_1/s_2 = 5$.

6. In order to estimate the rate of biochemical secretion at the head, $s_a(0)$, we suppose that each cell produces $\hat{s}_a$ molecules of biochemical each second. If the cells are closely packed with a cell length of 10 μm, this implies that

$$s_a(0) = \frac{\hat{s}_a\left(10^5\right)^3}{6\times 10^{23}}\ \text{mol m}^{-3}\text{s}^{-1} = \frac{\hat{s}_a}{6\times 10^{11}}\ \text{Ms}^{-1}.$$

A possible value for $\hat{s}_a$ is suggested by the production of receptors, which occurs at a fate of $k_i b$ when the binding kinetics are at equilibrium. Now $k_i \approx 2 \times 10^{-3}$ s^{-1}, and $b \sim 10^4$ per cell, so that new receptors are produced on the cell surface at a rate of about 20 receptors per cell per second. Intuitively we expect $\hat{s}_a$ to have roughly the same order of magnitude.

It is crucial to stress that these parameter estimations are very crude, and do no more than suggest approximate orders of magnitude. However, the qualitative forms of the numerical solutions presented in the main body of the paper are not unduly sensitive to any of the parameter values.

A.2. Nondimensionalisation

We nondimensionalize the model using the following dimensionless rescalings (* denotes a dimensionless quantity):

$$x^* = x/L \qquad t^* = \mu_a t \qquad a^* = a\mu_a / s_a(0) \qquad f^* = f/\alpha_1$$

$$b^* = b/\alpha_1 \qquad D_a^* = D_a / L^2\mu_a \qquad k_a^* = k_a s_a(0)/\mu_a^2 \qquad k_d^* = k_d/\mu_a$$

$$k_i^* = k_i/\mu_a \qquad \zeta^* = \zeta L \qquad \xi^* = \alpha_1\mu_a / s_a(0) \qquad \alpha_2^* = \alpha_2/\alpha_1$$

$$\beta^* = \beta \qquad e^* = e\mu_e / s_1 \qquad D_e^* = D_e / L^2\mu_a \qquad s_2^* = s_2 / s_1$$

$$\mu_e^* = \mu_e / \mu_a \qquad k_e^* = k_e s_1 / \mu_a \mu_e \qquad y^* = y / L \qquad s_a^*(x^*) = s_a(x) / s_a(0)$$

$$s_e^*(x^*) = s_e(x) / s_1 \qquad \alpha^*(x^*) = \alpha(x) / \alpha_1.$$

Substituting these rescalings into (1) and dropping the asterisks for notational simplicity gives the following dimensionless equations:

$$\frac{\partial a}{\partial t} = D_a \frac{\partial^2 a}{\partial x^2} + s_a(x) - a - k_e ae - \xi k_a af + \xi k_d b, \tag{A2a}$$

$$\frac{\partial f}{\partial t} = k_d b - k_a af + k_i\left[\alpha(x) + \beta b - f\right], \tag{A2b}$$

$$\frac{\partial b}{\partial t} = k_a af - (k_d + k_i)b, \tag{A2c}$$

$$\frac{\partial e}{\partial t} = D_e \frac{\partial^2 e}{\partial x^2} + \mu_e\left[s_e(x) - e\right] \tag{A2d}$$

where $s_e(x) = s_2 y(x) + 1 - y(x)$, $\alpha(x) = \alpha_2 y(x) + 1 - y(x)$, and $s_a(x) = 1$ for $0 < y(x) < 4/5$ and $5(1 - y(x))$ for $4/5 < y(x) < 1$. Based on the arguments discussed above, we use the following dimensionless parameter values in our simulations: $D_a = 0.04$, $k_e = 15$, $k_a = 8$, $\xi = 0.04$, $k_d = k_i = 10$, $\alpha_2 = s_2 = 0.2$, $\beta = 0.9$, $D_e = 0.04$, $\mu_e = 1$.

We solved the system (2) numerically using a semi-implicit finite difference scheme, that is, in the discretisation, the two diffusion terms were evaluated at the new time point, with all other terms on the right hand sides evaluated at the old time point. This reduces the equations to a tridiagonal system of linear equations at each time step. In our solutions we took the dimensionless initial conditions to be $a = b = e \equiv 0, f \equiv 1$; however, limited numerical investigation suggests that the final equilibrium is independent of the initial conditions.

REFERENCES

ANDO, H., SAWADA, Y., SHIMIZU, H. and SUGIYAMA, T. (1989) Pattern formation in *Hydra* tissue without developmental gradients, *Dev. Biol.*, **133**, 405–414.

BENSON, D. L., SHERRATT, J. A. and MAINI, P. K. (1993) Diffusion driven instability in an inhomogeneous domain, *Bull. Math. Biol.*, **55**, 365–384.

BERKING, S. (1977) Bud formation in *Hydra*: inhibition by an endogenous morphogen, *Roux's Arch. Dev. Biol.*, **181**, 215–225.

BERKING, S. (1984) Metamorphosis of *Hydractinia echinata*. Insights into pattern formation of hydroids, *Roux's Arch. Dev. Biol.*, **193**, 370–378.

BODE, P. M. and BODE, H. R. (1984) Patterning in *Hydra*, in *Pattern Formation: A Primer in Developmental Biology* (eds. G. M. Malacinski and S. V. Bryant) MacMillan Publ. Co., New York, pp. 213–241.

BODE, P. M., AWAD, T. A., KOIZUMI, O., NAKASHIMA, Y., GRIMMELIKHUIJZEN, C. J. and BODE, H. R. (1988) Development of the two part pattern during regeneration of the head in *Hydra*, *Development*, **102**, 223–235.

BURNETT, A. L. (1966) A model of growth and cell differentiation in *Hydra*, *Am. Nat.*, **100**, 165–189.

CAMPBELL, R. D. (1967) Tissue dynamics of steady state growth in *Hydra littoralis*. II. Patterns of tissue movement, *J. Morphol.*, **121**, 19–28.

GIERER, A. and MEINHARDT, H. (1972) A theory of biological pattern formation, *Kybernetik*, **12**, 30–39.

GIERER, A., BERKING, S., BODE, H., DAVID, C. N., FLICK, K., HANSMANN, G., SCHALLER, H. and TRENKNER, E. (1972) Regeneration of *Hydra* from reaggregated cells, *Nature New Biol.*, **239**, 98–101.

GIERER, A. (1977) Biological features and physical concepts of pattern formation exemplified by *Hydra*, *Dev. Biol.*, **138**, 243–245.

HÖFER, T., MAINI, P. K., SHERRATT, J. A., CHAPLAIN, M. A. J., CHAUVET, P., METEVIER, D., MONTES, P. C. and MURRAY, J. D. (1994) A resolution of the chemotactic wave paradox, *Appl. Math. Lett.*, **7**, 1–5.

MACWILLIAMS, H. K. (1982) Numerical simulations of *Hydra* head regeneration using a proportion-regulating version of the Gierer-Meinhardt model, *J. Theor. Biol.*, **99**, 681–703.

MACWILLIAMS, H. K. (1983a) *Hydra* transplantation phenomena and the mechanism of *Hydra* head regeneration. I. Properties of the head inhibition, *Dev. Biol.*, **96**, 217–238.

MACWILLIAMS, H. K. (1983b) *Hydra* transplantation phenomena and the mechanism of *Hydra* head regeneration. II. Properties of the head activation, *Dev. Biol.*, **96**, 239–257.

MAINI, P. K., BENSON, D. L. and SHERRATT, J. A. (1992) Pattern formation in reaction-diffusion models with spatially inhomogeneous diffusion coefficients, *IMA J. Math. Appl. Med. Biol.*, **9**, 197–213.

MARTIEL, J.-L. and GOLDBETER, A. (1987) A model based on receptor desensitization for cyclic AMP signalling in *Dictyostelium* cells, *Biophys. J.*, **52**, 807–828.

MEINHARDT, H. and GIERER, A. (1974) Applications of a theory of biological pattern formation based on lateral inhibition, *J. Cell Sci.*, **15**, 321–346.

MEINHARDT, H. (1993) A model for pattern formation of hypostome, tentacles and foot in *Hydra*: how to form structures close to each other, how to form them at a distance, *Dev. Biol.*, **157**, 321–333.

MENDELSOHN, C., RUBERTE, E., LEMEUR, M., MORRISS-KAY, G. and CHAMBON, P. (1991) Developmental analysis of the retinoic acid inducible RAR-β2 promotor in transgenic animals, *Development*, **113**, 723–734.

MONK, P. B. and OTHMER, H. G. (1989) Cyclic AMP oscillations in suspensions of *Dictyostelium discoideum*, *Phil. Trans. R. Soc. Lond.*, **B323**, 185–224.

MORGAN, T. H. (1904) An attempt to analyse the phenomena of polarity in *Tubularia*, *J. Exp. Zool.*, **1**, 587–591.

MÜLLER, W. A. (1982) Intercalation and pattern regulation in hydroids, *Differentiation*, **22**, 141–150.

MÜLLER, W. A. (1989) Diacylglycerol-induced multiheaded formation in *Hydra*, *Development*, **105**, 309–316.

MÜLLER, W. A. (1990) Ectopic head and foot formation in *Hydra*: diacylglycerol-induced increase in positional value and assistance of the head in foot formation, *Differentiation*, **42**, 131–143.

MÜLLER, W. A. (1993) Pattern control in *Hydra*: basic experiments and concepts, in *Experimental and Theoretical Advances in Biological Pattern Formation* (eds. H. G. Othmer, P. K. Maini and J. D. Murray) Plenum Press, New York.

MÜLLER, W. A. (1995a) Competition for factors and cellular resources as a principle of pattern formation in *Hydra*. I. Increase of the potentials for head and bud formation and rescue of the regeneration-deficient mutant *reg*-16 by treatment with diacylglycerol and arachidonic acid, *Dev. Biol.*, **167**, 159–174.

MÜLLER, W. A. (1995b) Competition for factors and cellular resources as a principle of pattern formation in

Hydra. II. Assistance of foot formation by heads and buds and a new model of pattern control, *Dev. Biol.*, **167**, 175–189.

NODA, K. (1971) Reconstitution of dissociated cells of *Hydra*, *Zool. Mag.*, **80**, 99–101.

NOJI, S., NOHNO, T., KOYAMA, E., MUTO, K., OHYAMA, K., AOKI, Y., TAMURA, K., OHSUGI, K., IDE, H., TANIGUCHI, S. and SAITO, T. (1991) Retinoic acid induces polarising activity but is unlikely to be a morphogen in the chick limb bud, *Nature*, **350**, 83–86.

SATO, M., TASHIRO, H., OIKAWA, A. and SAWADA, Y. (1992) Patterning in *Hydra* cell aggregates without sorting of cells from different axial origins, *Dev. Biol.*, **151**, 111–116.

SHERRATT, J. A. (1994) Chemotaxis and chemokinesis in eukaryotic cells: the Keller-Segel equations as an approximation to a detailed model, *Bull. Math. Biol.*, **56**, 129–146.

SHERRATT, J. A. and MURRAY, J. D. (1990) Models of epidermal wound healing, *Proc. R. Soc. Lond.*, **B241**, 29–36.

SHERRATT, J. A., SAGE, H. E. and MURRAY, J. D. (1993) Chemical control of eukaryotic cell movement: a new model, *J. Theor. Biol.*, **162**, 23–40.

SKLAR, L. A., FINNEY, D. A., OADES, Z. G., JESAITIS, A. J., PAINTER, R. G. and COCHRANE, C. G. (1984) The dynamics of ligand-receptor interactions, *J. Biol., Chem.*, **259**, 5661–5669.

TECHNAU, U. and HOLSTEIN, T. W. (1992) Cell sorting during the regeneration of *Hydra* from reaggregated cells, *Dev. Biol.*, **151**, 117–127.

TREMBLEY, A. (1744) Mémories, pour servir à l'histoire d'un genre polypes d'eau douce, à bras en forme de cornes. Verbeek, Leiden. A fascinating acount of Trembley's pioneering work on *Hydra* is given by J. R. Baker (1952) "Abraham Trembley of Geneva: Scientist and Philosopher", Edward Arnold, London.

TURING, A. M. (1952) The chemical basis of morphogenesis, *Phil. Trans. R. Soc. Lond.*, **B237**, 37–72.

WEBSTER, G. and WOLPERT, L. (1966) Studies on pattern regulation in *Hydra*. I. Regional differences in time required for hypostome determination, *J. Embryol. Exp. Morph.*, **16**, 91–104.

WOLPERT, L. (1969) Positional information and the spatial pattern of cellular differentiation, *J. Theor. Biol.*, **25**, 1–47.

WOLPERT, L., HORNBRUCH, A. and CLARKE, M. R. B. (1974) Positional information and positional signalling in *Hydra*, *Am. Zool.*, **14**, 647–663.

ZIMMER, A. and ZIMMER, A. (1992) Induction of RARβ2-lacZ transgene by retinoic acid reflects the neuromeric organisation of the central nervous system, *Development*, **116**, 977–983.